Journal of Theoretical and Applied Information Technology
28th February 2025. Vol.103. No.4

ISSN: 1992-8645 www.jatit.org E-ISSN: 1817-3195

BTLBD - A FUSION OF CNN, LSTM, AND BIGRU MODEL WITH IMAGE DATA AUGMENTATION FOR IMPROVED BRAIN TUMOR DIAGNOSIS USING OPTIMIZATION

YENUMALA SANKARARAO[1] AND SYED KHASIM[2]

[1, 2] School of Computer Science and Engineering, VIT-AP University, Amaravati,
Andhra Pradesh 522237, India

Email:[1]y.sankar123@gmail.com,[2]profkhasim@gmail.com
Corresponding author Email: profkhasim@gmail.com

ABSTRACT

The pressing need for accurate and timely diagnosis of brain tumors underscores the importance of advancing diagnostic technologies. Traditional methods, though effective to a degree, often fall short in terms of precision, accuracy, and speed, crucial factors in brain tumor identification and treatment. This work acknowledges these limitations by introducing a novel deep learning model that identifies brain tumors within a multiclass classification framework. Existing methodologies in brain tumor detection often struggle with lower precision, accuracy, and recall, alongside higher delay times in diagnosis. These shortcomings can lead to significant impacts on patient outcomes, where early and accurate diagnosis is paramount. The Convolution Normalization Mean Filter (CNMF) filter and generative adversarial networks (GAN) for preprocessing are used in a special way in our proposed model to get around these problems. GANs are particularly beneficial in expanding the size of a dataset. The CNMF Filter is a technique for smoothing and reducing noise in images. Fuzzy saliency maps for segmentation. After segmentation, PCA extracts features from the segmented MRI images. We employ the Horse Head Optimization (HHO) technique to select the most optimal features. Finally, we perform classification using a fusion of CNN, LSTM, and BiGRU models. The effectiveness of our model is evident when tested on a dataset containing four brain tumor classes: meningioma, glioma, pituitary, and no tumor. The results demonstrate a significant improvement over existing methods; the proposed model's accuracy in diagnosis is 97.19%, and its accuracy with augmentation is 98.95%. The impacts of this work are far-reaching. By improving the precision and speed of brain tumor diagnosis, our model not only enhances the prospects for timely and effective treatment but also reduces the emotional and financial burdens on patients and healthcare systems. Furthermore, this study's developed methodology establishes a new standard in medical imaging analysis, potentially opening the door for its use in other intricate diagnostic tasks. This work represents a significant step forward in the intersection of deep learning and medical diagnostics, offering a promising tool in the fight against brain tumors.

Keywords: *Brain Tumor Detection, Deep Learning, Recurrent Convolutional Neural Network, Generative Adversarial Networks, Fuzzy Saliency Maps.*

1. INTRODUCTION

The field of clinical imaging has seen a substantial revolution with the advent of deep learning technologies, particularly in the detection and analysis of brain tumors. Brain tumors, ranging from benign to malignant types like meningiomas, gliomas, and pituitary tumors, pose significant diagnostic challenges due to their varied appearances and growth patterns. Precise and prompt diagnosis is crucial for efficient treatment planning. making advancing diagnostic tools a key focus in medical research.

Traditional diagnostic methods, while foundational, are increasingly seen as inadequate in addressing the complexities inherent in brain tumor identification. Issues such as lower precision and accuracy, delayed diagnosis, and difficulties in distinguishing between tumor types have highlighted the need for more sophisticated and efficient tools. The introduction of deep learning in medical imaging has opened new avenues for addressing these challenges, offering enhanced

capabilities in pattern recognition, feature extraction, and image analysis.

The inclusion of deep learning models such as convolutional neural networks (CNNs) has greatly improved the examination of medical imaging data. However, the quality of the input data and its capacity to understand temporal and geographic interconnections within the images frequently limit the effectiveness of these models. Addressing these limitations necessitates a more nuanced approach that not only refines the input data but also leverages the strengths of various deep learning architectures.

This study shows a new type of deep learning model that uses generative adversarial networks (GANs) for preprocessing and a CNMF filter to deal with these problems. Fuzzy Saliency Maps for segmentation. This approach enhances the input data quality, allowing for a more detailed and accurate feature extraction process. Central to our model is the fusion of CNN, Long Short-Term Memory (LSTM) networks and Bidirectional Gated Recurrent Units (BiGRU) . The functions of both recurrent and convolutional models are used in these fusion processes. This lets the model extract combined temporal and spatial dependencies in the imaging data more efficiently.

The proposed model is a significant advancement over existing methods, offering higher precision, accuracy, recall, and specificity in brain tumor identification. By overcoming the drawback of traditional diagnostic tools, this model not only improves diagnostic outcomes additionally, It improves our understanding of the use of deep learning in medical imaging.

. This paper aims to detail the development and validation of this model, highlighting its potential impact on the field of medical diagnostics and beyond.

1.1 Motivation & Contribution:

Motivation:

The impetus for this research stems from the urgent need to enhance brain tumor diagnosis, which remains a critical challenge in medical imaging. Brain tumors, due to their diverse types and characteristics, demand precise and rapid identification for effective treatment. The motivation behind this work is threefold: The objective is to overcome the restrictions of existing diagnostic techniques, utilize the capabilities of deep learning in medical imaging, and enhance patient outcomes by using new technical solutions.

Current diagnostic methods, including MRI and CT scans, are fundamental but often lack the precision and speed necessary for optimal brain tumor diagnosis. These limitations can lead to delayed or inaccurate treatment decisions, adversely affecting patient outcomes. The complexity and variability of brain tumors require a diagnostic tool that is not only accurate but also efficient in handling diverse data and capable of distinguishing between different tumor types.

Bridging Technological and Clinical Practices: By integrating advanced deep learning techniques into medical imaging, our work bridges the gap between technological innovation and clinical application. This integration has the potential to transform diagnostic practices, making them more efficient and accurate.

Setting New Benchmarks in Medical Imaging Analysis: The methodology and results presented in this paper set new benchmarks in the field of medical imaging analysis. The model not only demonstrates its effectiveness in brain tumor detection but also opens avenues for its application in other complex diagnostic tasks, potentially revolutionizing the approach to medical diagnostics.

In summary, this work not only addresses the critical challenges in brain tumor diagnosis but also contributes to the broader field of medical imaging and deep learning. The advancements presented in this paper have the potential to significantly impact clinical practices, leading to improved patient care and outcomes.

Contribution:

- This study presents numerous significant advances in medical imaging and brain tumor diagnosis. Advanced Preprocessing Techniques: We introduce an innovative preprocessing method using Generative Adversarial Networks (GANs) and CNMF Filter combined with Fuzzy Saliency Maps. This approach significantly enhances the quality of imaging data, leading to improved feature extraction and analysis.
- After segmentation, PCA extracts features from the segmented MRI images. We employ the Horse Head Optimization (HHO) technique to select the most optimal features
- Fusion of Deep Learning Architectures: Our model uniquely integrates Convolutional Neural Networks (CNNs)

and Long Short-Term Memory (LSTM) networks with Bidirectional Gated Recurrent Units (BiGRU) .This fusion capitalizes on the strengths of both recurrent and convolutional architectures, enabling the model to effectively capture complex temporal and spatial patterns in brain imaging data.

- Improved Diagnostic Metrics: The proposed model demonstrates superior performance in diagnosing brain tumors, as evidenced by significant improvements in precision, accuracy, recall, specificity, and reduced diagnostic delay. These advancements are critical in clinical settings, where timely and precise diagnosis can have a significant impact on the patient's treatment effectiveness and prognosis.

The use of GANs for synthetic data generation introduces the risk of producing unrealistic or biased samples, which could affect model generalization. The model's performance may vary significantly with different hyper parameter settings, potentially affecting reproducibility. The application of the Horse Head Optimization (HHO) technique for feature selection may not always guarantee the selection of the most relevant features for all datasets.

Performance Metrics They are justified by their importance in measuring model accuracy, precision, recall, and general effectiveness. We compared the study against recent literature to ensure a competitive evaluation.

The importance of IT research in this study is evident in its potential to revolutionize brain tumor diagnosis through automated, high-precision deep learning algorithms. Traditional diagnostic methods rely on manual radiological assessment, which is time-consuming and prone to human error. This research advances IT contributions by:

Enhancing Diagnostic Accuracy:

The model ensures a more accurate and faster diagnosis by using deep learning techniques (CNN, LSTM, and BiGRU) and choosing the best features. This lowers the chance of wrong classification. This research establishes a deep learning framework that can be deployed as a Clinical Decision Support System (CDSS) in hospitals, aiding radiologists and reducing the burden on healthcare systems.

2. REVIEW OF EXISTING MODELS FOR CLASSIFICATION OF BRAIN TUMORS

The recent advancements in brain tumor detection, segmentation, and analysis using machine learning and deep learning techniques have shown significant potential in improving diagnostic accuracy and patient outcomes. This literature review examines key contributions in this field, focusing on the application of various computational methods to magnetic resonance imaging (MRI) data samples.

Shah et al. [1] The study presented a strong approach to identify brain tumors using a refined EfficientNet model, which demonstrated enhanced effectiveness in identifying tumors in MRI pictures. This research corresponds with the increasing trend of utilizing deep learning models for medical imaging analysis. Similarly, Ezhov et al. [2] explored a geometry-aware neural solver for the fast Bayesian calibration of brain tumor models, highlighting the importance of incorporating geometric information in model development. Ahmad and Choudhury [3] The study explored the efficacy of deep transfer learning networks in detecting brain tumors using MR images. Their findings underscore the effectiveness of transfer learning in medical imaging tasks, where large-scale data is often unavailable. Kujur et al. [4] made a significant contribution by evaluating how the model relies on brain MRI images for classification, focusing on the complexity of data and its impact on model performance, which is crucial for understanding the limitations and capabilities of different algorithms. Ferdous et al. [5] introduced LCDEiT, a linear complexity data-efficient image transformer, tailored for MRI brain tumor classification. Their work represents a significant step towards efficient and accurate image-based diagnosis. Rahimpour et al. [6] we investigated cross-modal distillation as a means to enhance MRI-based brain tumor segmentation when certain MRI sequences are absent, addressing a common challenge in medical imaging where complete data sets are not always available. In a novel approach, Bs et al. [7] and BS et al. [8] investigated the electrical phenotyping of human brain tissues for tumor delineation, showcasing the potential of alternative methods in tumor identification and characterization. Mohsen et al. [9] combined hybrid single image super-resolution techniques with advanced pre-trained models for brain tumor classification, emphasizing the synergy between high-resolution imaging and deep learning models. Renugadevi et al. [10] introduced a model that uses machine learning to segment and grade brain tumors. Our model specifically focuses on predicting patients' lifespans, which is critical for

determining their prognosis and arranging their treatment. Zhuang et al. [11] developed a 3D cross-modality feature interaction network that aligns volumetric features for the segmentation of brain tumors and tissues. This highlights the significance of using 3D imaging techniques to accurately capture the intricate characteristics of brain tumors. Lin et al. [12] CKD-TransBTS is a novel hybrid transformer model that utilizes clinical knowledge to improve brain tumor segmentation. It incorporates modality-correlated cross-attention to enhance the accuracy of the segmentation process, illustrating the integration of clinical expertise with advanced computational models. Subramanian et al. [13] Research primarily focuses on ensemble inversion techniques for brain tumor development models with mass effects. This research aims to enhance our understanding of the dynamics of tumor growth and its implications for treatment. Lastly, Cheng et al. [14], Zaitoon, and Syed [15] explored innovative approaches to brain tumor treatment and prognosis. Cheng et al. The researchers did a study on what happened when they used MR-guided focused ultrasound to open the blood-brain barrier and apply localized mild hyperthermia to the brain at the same time. Meanwhile, Zaitoon and Syed developed RU-Net2+, a deep learning system that accurately segments brain tumors and predicts survival rates. Zhao et al. [16] investigated an uncertainty-aware multi-dimensional mutual learning approach for brain and brain tumor segmentation. Their work underscores the importance of handling uncertainty in medical imaging, a critical factor for reliable diagnosis. Ottom et al. [17] developed Znet, a deep learning model for 2D MRI brain tumor segmentation, which demonstrates the effectiveness of deep learning in processing two-dimensional medical images.

Ramprasad et al. [18] introduced SBTC-Net, a secured brain tumor segmentation and classification system, incorporating black widow and genetic optimization algorithms. This study highlights the growing trend of integrating advanced optimization techniques in medical imaging analysis. Ding et al. [19] introduced the MVFusFra framework as a method for segmenting brain tumors using several views and modalities to improve accuracy. Sekhar et al. [20] This study primarily categorizes brain tumors using optimized GoogleNet characteristics and machine learning techniques. This demonstrates the pragmatic use of transfer learning in medical imaging. Chen et al. [21] improved contrast in MR images using 3D high-resolution convolutional neural networks (ConvNets), a critical step in enhancing the clarity and distinguishing tumor tissues in MRI scans. Solanki et al. [22] provided an overview of brain tumor detection and classification using intelligence techniques, summarizing the current state and advancements in this field. Alagarsamy et al. [23] created an automated system for segmenting brain tumors in MR brain pictures by combining an artificial bee colony with an interval type II fuzzy technique. This demonstrates the effectiveness of bio-inspired algorithms in analyzing medical images.Yan et al. [24] introduced SEResU-Net for multimodal brain tumor segmentation, emphasizing the importance of incorporating advanced neural network architectures for improved segmentation performance. Jabbar et al. [25] proposed a hybrid Caps-VGGNet model for brain tumor detection and multi-grade segmentation, illustrating the effectiveness of combining different neural network architectures for complex tasks like tumor grading. Yang et al. [26] presented a flexible fusion network for multi-modal brain tumor segmentation, addressing the challenge of integrating diverse imaging modalities for comprehensive analysis. Ravendra et al. [27] we have optimized GoogleNet characteristics and machine learning techniques. This demonstrates the pragmatic use of transfer learning in medical imaging. Ismail et al. [28] focused on radiomic deformation and textural heterogeneity descriptors to characterize tumor field effects, particularly in glioblastoma, linking imaging features with survival prediction. Metlek and Çetıner [29] proposed ResUNet+, a new convolutional and attention block-based approach for brain tumor segmentation, highlighting the ongoing innovation in neural network design for medical applications. Finally, Farzamnia et al. [30] investigated MRI brain tumor detection methods using contourlet transform based on a time-adaptive self-organizing map, showcasing the integration of traditional image processing techniques with modern neural networks.

In this study, we present a complete deep learning model that combines advanced preprocessing methods, feature extraction, and a hybrid classification framework. This approach has demonstrated notable accuracy improvements, achieving 97.19% without augmentation and 98.95% with augmentation.

In summary, these studies collectively advance the field of brain tumor analysis through the application of sophisticated computational techniques. They showcase the capabilities of machine learning and deep learning in improving the precision,

effectiveness, and dependability of brain tumor detection, segmentation, and classification. This, in turn, leads to better diagnostic procedures and patient care results. Table 1 provides a comprehensive review of existing methods.

Table 1. Review of existing methods.

Ref. No.	Name of Method	Advantages	Limitations	Details of Work	Future Scope
[1]	Finetuned EfficientNet	High robustness in detection	May require large datasets for fine-tuning	Brain tumor detection in MRIs	Explore other medical imaging modalities
[2]	Geometry-Aware Neural Solver	Fast Bayesian calibration	Specific to brain tumor models	Calibration of brain tumor models using geometry-aware techniques	Integration with other diagnostic tools
[3]	Deep Transfer Learning Networks	Effective for MR image analysis	Dependence on pre-trained models	Utilizes transfer learning for tumor detection	Enhancing model adaptability to new datasets
[4]	Data Complexity Evaluation	Addresses model dependence issues	May not generalize well	Evaluates model dependence in brain MRI image classification	Further refinement of evaluation techniques
[5]	LCDEiT	Linear complexity, data-efficient	Limited to MRI brain tumor classification	Image transformer technique for MRI brain tumor classification	Application to other types of medical imaging
[6]	Cross-Modal Distillation	Improves segmentation with missing sequences	Requires multiple MRI sequences	Utilizes cross-modal learning for tumor segmentation	Refinement of distillation techniques
[7]	Automated System for Tumor Delineation	High precision in delineation	Limited to electrical phenotyping	Electrical phenotyping for brain tumor delineation	Exploration of additional delineation methods
[8]	Hybrid SISR Technique	Combines ResNext101_32×8d and VGG19 models	May require high computational resources	Uses super-resolution and pre-trained models for classification	Application in other forms of cancer detection
[9]	ML-Based Segmentation and Grading	Lifetime prediction capability	Specific to machine learning models	Employs ML for tumor segmentation and grading	Extension to other diseases and conditions
[10]	3D Cross-Modality Network	Effective in feature alignment	Complexity in 3D analysis	Utilizes volumetric feature alignment for segmentation	Expansion to 2D and 4D imaging techniques
[11]	Electromechanical Characterization	Potential biomarker identification	Requires extensive validation	Characterizes brain tissues for tumor delineation	Clinical implementation and further

					validation
[12]	CKD-TransBTS	Incorporates clinical knowledge	May not generalize across all tumor types	Hybrid transformer with modality-correlated attention for segmentation	Broader application in medical imaging
[13]	Ensemble Inversion	Addresses tumor growth models	Complexity in implementation	Inversion technique for brain tumor growth models	Refinement and simplification of the method
[14]	MR-Guided Focused Ultrasound	Simultaneous treatment and diagnosis	Limited to localized hyperthermia	Combines hyperthermia and barrier opening for treatment	Broader applicability in other brain disorders
[15]	RU-Net2+	High accuracy in segmentation	Limited to specific algorithm performance	Deep learning algorithm for tumor segmentation and survival prediction	Improving algorithm efficiency
[16]	Uncertainty-Aware Multi-Dimensional Learning	Addresses segmentation uncertainty	Complexity in learning approach	Multi-dimensional learning for brain tumor segmentation	Enhancing accuracy and reducing uncertainty
[17]	Znet	Deep learning approach	Specific to 2D MRI images	2D MRI brain tumor segmentation using deep learning	Extension to 3D and 4D imaging
[18]	SBTC-Net	Secured segmentation and classification	Requires specific optimization techniques	Brain tumor segmentation with genetic optimization	Further security enhancements in IoMT
[19]	MVFusFra	Multi-view dynamic fusion	Limited to multimodal segmentation	Dynamic fusion framework for multimodal brain tumor segmentation	Extension to single-modal imaging
[20]	Fine-Tuned GoogLeNet Features	Utilizes machine learning algorithms	Reliant on fine-tuning for specific tasks	Classification using fine-tuned GoogLeNet features	Exploration of other deep learning models
[21]	3D High-Resolution ConvNets	Effective in contrast enhancement	High computational demand	Synthesizes MR image contrast using ConvNets	Application to other imaging techniques
[22]	Overview of Intelligence Techniques	Comprehensive review	Limited to existing techniques	Overview and classification of brain tumor detection techniques	Identification of new intelligence techniques
[23]	ABC Combined with Fuzzy Technique	Automated segmentation	Specific to brain MR images	Uses artificial bee colony and fuzzy technique for segmentation	Refinement and optimization of the method
[24]	SEResU-Net	Effective for multimodal	May require	Multimodal brain tumor	Application in real-time

		segmentation	extensive training	segmentation using SEResU-Net	diagnosis
[25]	Hybrid Caps-VGGNet Model	Effective in multi-grade segmentation	Requires large datasets for training	Detects and segments brain tumors using hybrid model	Exploring other hybrid deep learning models
[26]	Flexible Fusion Network	Addresses multi-modal segmentation	Complexity in network design	Multi-modal brain tumor segmentation	Simplifying the network for broader use
[27]	Automated Segmentation Using Deep Learning	High automation	May lack generalizability	Deep learning for automated segmentation of brain MRI images	Expanding to other types of tumors
[28]	R-DepTH Descriptor	Characterizes tumor field effect	Specific to glioblastoma	Radiomic descriptor for survival prediction in glioblastoma	Application to other cancer types
[29]	ResUNet+	Utilizes convolutional and attention blocks	Specific to brain tumor segmentation	New approach for brain tumor segmentation	Adapting to other medical conditions
[30]	Contourlet Transform Based Detection	Time adaptive self-organizing map	Specific to MRI brain tumors	Brain tumor detection using contourlet transform	Application in other imaging modalities

3. PROPOSED DESIGN FOR IMPROVING THE EFFICIENCY OF BRAIN TUMOR DIAGNOSIS.

To overcome issues of low efficiency and limited scalability with existing models, the Brain Tumor Location and Boundary Detection (BTLBD) model fuses cutting-edge deep learning methods are applied in medical imaging, forging a new path in Identifying brain tumors in their earliest stages with accuracy is crucial. As per Figure 1, at its core, the BTLBD model ingeniously melds the strengths of the robust feature extraction capabilities of Convolutional Neural Networks (CNNs), Long Short-Term Memory (LSTM) and Bidirectional Gated Recurrent Units (BiGRU). The diagram appears to outline a multi-step pipeline for brain tumor classification using MRI images. It includes several key stages: preprocessing, segmentation, feature extraction, and classification. The process begins with MRI images of the brain, which are the raw input for the system.

The preprocessing phase involves two techniques aimed at preparing the images for further analysis: Constrained non-negative matrix factorization (CNMF) filter: This filter likely reduces noise, improves image quality, and extracts meaningful features from MRI scans. Here, we use generative adversarial networks (GANs) to enhance image quality or produce synthetic data that facilitates improved segmentation and feature extraction. GANs can help create more robust models by augmenting data or refining images. After preprocessing, the images go through segmentation, which uses fuzzy saliency maps [31]. Fuzzy Saliency Maps: These maps highlight the most important regions of the MRI images (in this case, tumor regions), making the segmentation more accurate by focusing on regions of interest, such as tumors or abnormal areas.The feature extraction stage then receives the segmented and preprocessed images. This stage uses CNN (convolutional neural networks), LSTM (long short-term memory), and BiGRU (bidirectional gated recurrent unit) to extract relevant features from the MRI images.

CNN extracts spatial features, such as edges and textures from the images.

LSTM and BiGRU: These models capture sequential or temporal relationships between features, thereby enhancing the ability to recognize patterns in image data. Finally, the system uses the extracted features to classify the MRI into one of four categories. Meningioma, Pituitary,Glioma, No Tumor

These fusions harness the CNN layers adeptly extract and analyze spatial features, making the

model exceptionally sensitive to the subtle nuances in medical images & samples. Simultaneously, LSTM's proficiency in capturing temporal dependencies and BiGRU's efficiency in processing data in both forward and reverse directions, ensuring comprehensive analysis of complex patterns in MRI scans.

As per Figure. 2. Such a configuration not only elevates the model's precision in classifying various brain tumor types but also significantly enhances its speed and accuracy, making it a beacon of innovation in the realm of medical diagnostics. The BTLBD model, therefore, stands as a testament to the transformative potential of AI in healthcare, promising to revolutionize brain tumor diagnostics with its precision, efficiency, and reliability levels.

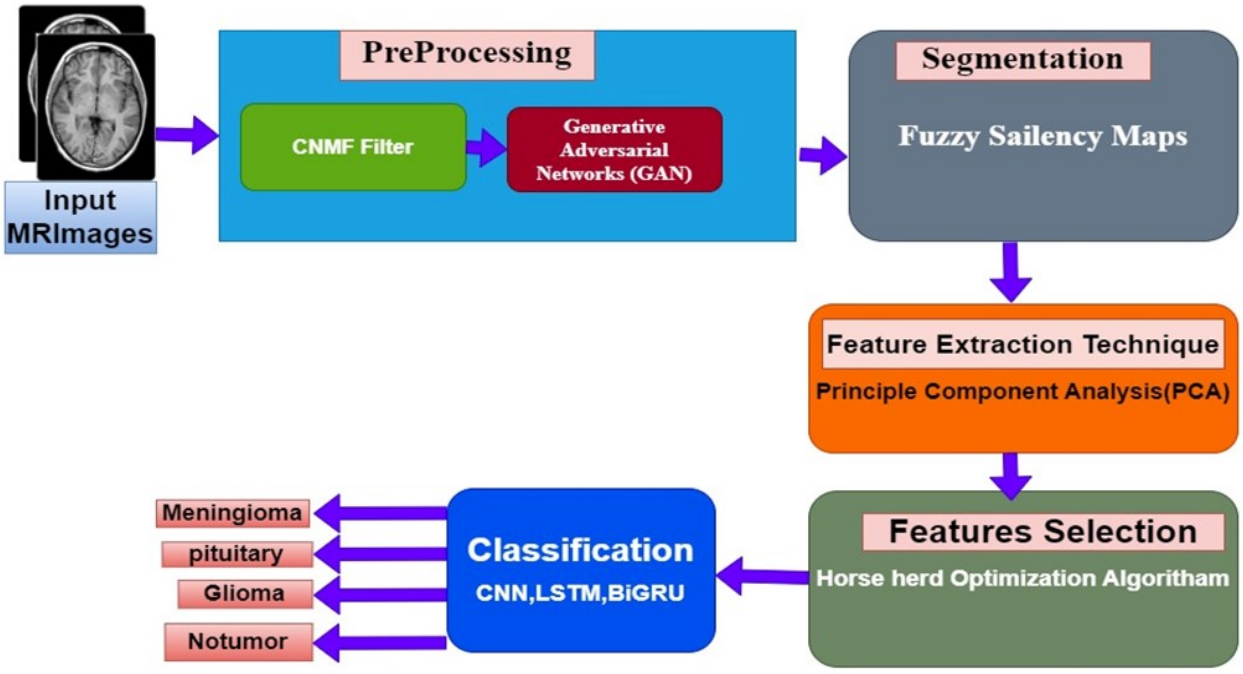

Figure 1. Proposed Architecture BTLBD Model.

Journal of Theoretical and Applied Information Technology
28th February 2025. Vol.103. No.4

ISSN: 1992-8645 www.jatit.org E-ISSN: 1817-3195

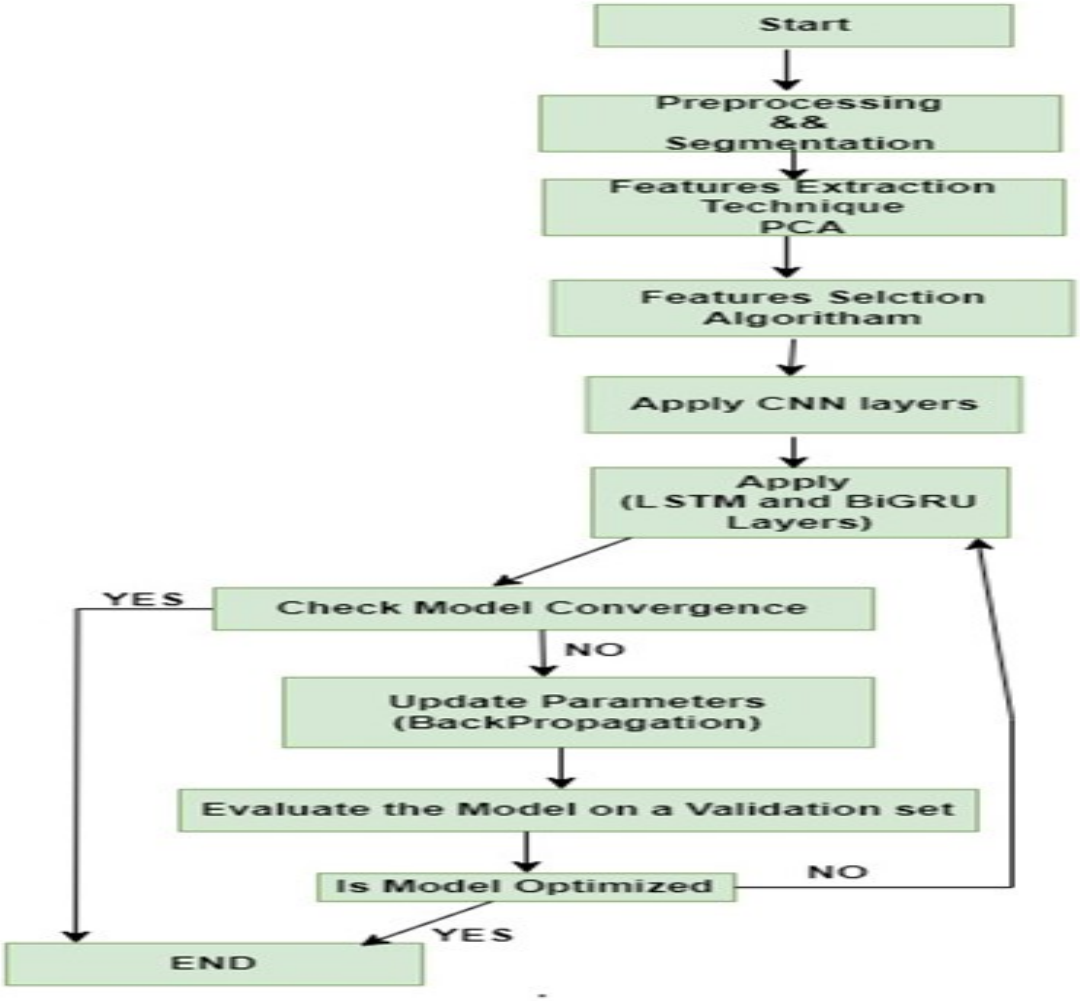

Figure.2. Data Flow Of The Training Process Of The BTLBD Model.

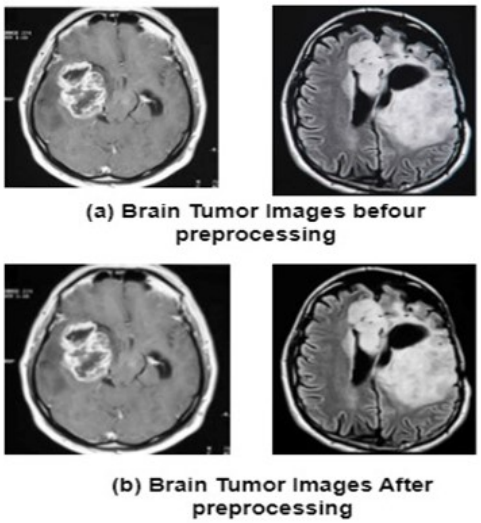

Figure:3 (A) Original Images (B) Pre-Processing Images.

Journal of Theoretical and Applied Information Technology
28th February 2025. Vol.103. No.4

ISSN: 1992-8645 www.jatit.org E-ISSN: 1817-3195

3.1 Preprocessing- CNMF Filter:

Figure 3:(a) The original set of images before any modifications; (b) The images after undergoing the pre-processing steps, which include noise reduction. Image processing uses the robust and adaptable Convolution Normalization Mean Filter (CNMF). Through the integration of convolution, mean filtering, and normalization, CNMF efficiently reduces noise, improves characteristics, and readies images for subsequent analysis. Nevertheless, meticulous deliberation is necessary concerning the size and form of the kernel in order to achieve a harmonious optimization of noise reduction and detail.

Convolution: Convolution is a mathematical procedure in signal processing, including image processing, that filters data or extracts specific information. In the context of image processing, convolution encompasses the subsequent stages:

A kernel, also known as a filter, is a compact matrix or mask selected to specifically achieve a certain filtering effect, such as edge detection or blurring. The typical dimensions of a kernel are 3x3, 5x5, or 7x7 pixels, although they may differ based on the specific implementation.

The sliding window operation involves incrementally moving the kernel over the image, pixel by pixel. At every locus, the kernel values undergo multiplication with the corresponding pixel values present in the image. We then aggregate the products to calculate a new pixel value for the output image.

The convolution technique yields a new image that highlights specific characteristics based on the selected kernel. For example, a sharpening kernel will optimize the sharpness of edges, whereas a smoothing kernel will minimize the presence of noise.

Mathematically, the convolution of an image I with a kernel K can be expressed as.

$$(I * K)(x,y) = \sum_{i=-m}^{m} . \sum_{j=-n}^{n} I(x+i, y+j).k(i,j)$$

Where: (x, y) is the position in the image,

I (x+i, y+j) denotes the pixel value at the coordinates (x+i, y+j).

The notation for the kernel value at (i, j) is K (i, j).

m and n define the kernel size (e.g., m=1, n=1for a 3x3 kernel).

3.1.1 normalization

Normalization refers to the procedure of rescaling pixel values to fit inside a predetermined range, usually [0, 1] or [0, 255] for pictures. The pixel values after the convolution procedure may surpass the standard range as a result of the buildup of sums, particularly when using larger kernels or high-intensity regions. Normalization is implemented on:

- Maintain Pixel Range: Ensures that the pixel values remain within the displayable range.
- Enhance Contrast: Improves the contrast of the image by spreading the values more evenly.
- Standardize Data: Makes it easier to compare different images or apply further image processing techniques.

Normalization is usually done using the formula:

$$I_{normalized}(x,y) = \frac{I(x,y) - I_{min}}{I_{max} - I_{min}}$$

I (x, y) is the pixel value,

I min stands for the minimum pixel value in the image.

I max stand for the maximum pixel value in the image.

3.1.2 mean filtering

A linear filter known as mean filtering, or averaging filter, smooths an image by minimizing the density of intensity fluctuations across adjacent pixels. People commonly use it to reduce noise. A mean filter operates by substituting each pixel's value with the average value of the pixels in its surrounding cluster.

For a 3x3 mean filter, the kernel looks like:

$$K = \frac{1}{9}\begin{bmatrix} 1 & 1 & 1 \\ 1 & 1 & 1 \\ 1 & 1 & 1 \end{bmatrix}$$

Algorithm: Pseudo-code for CNMF

Function CNMF (I , k_conv,k_mean):

M,N=Dimensions of I

I_conv=Zero Matrix of size M x N

I_mean=Zero Matrix of size M x N

I_final=Zero Matrix of size M x N

//Step 1: Convolution

For x=1 to M:

For y=1 to N:

Sum=0

For i= -m to m:

For j = -n to n:

If(x+i, y+j) is with in image bounds

Sum+=I(x+i, y+j)*k_conv(i,j)

I_conv(x,y)=sum

//step 2: Mean Filtering

For x=1 to M:

For y= 1 to N:

Sum=0

For i= -w/2 to w/2:

For j= -h/2 to h/2:

If(x+i, y+j) is with in image bounds

Sum+=I(x+i, y+j)

I_ mean (x, y) =Sum/(w*h)

// Step 3 : Normalization

I_ min = Min Value of I_mean

I_max=Max Value of I_mean

For x=1 to M:

For y=1 to N:

I_ final (x , y)=(I_mean(x,y)- I_ min) /(I_ max-I_ min)*255

Return I_ final

3.2 GAN

The GAN consists of two primary components: the Generator (G) and the Discriminator (D). The generator's objective is to create images that are indistinguishable from authentic MRI images, whereas the discriminator seeks to differentiate between genuine images (acquired MRI scans) and their synthetic counterparts across several samples.

The Generator takes in a random noise vector z sampled from a normal distribution. It uses G(z;θg) as its generator function, where θg represents the parameters of the Generator. The generator outputs Synthetic MRI images that mimic the distribution of real MRI scans. The generator's aim is to reduce the disparity between the distribution of generated images and that of real images, as articulated in equation 1.

$$ImageG(z;\theta g) = Augmented\ Synthetic\ MRI\ Imag \quad (1)$$

The Discriminator receives either a real MRI image or a synthetic image from the Generator. It uses D(x;θd) as the discriminating function, where θd are the parameters of the Discriminator and x represents the input image scans. It generates a probability score indicating the chance that the input image is an authentic MRI scan. This is done to maximize its ability to correctly classify real and synthetic images & samples, which is represented via equation 2,

$$D(x;\theta d)=P(Real(MRI)) \quad (2)$$

The training involves a min-max game where the Generator and Discriminator are trained simultaneously. The primary objective of the generator is to deceive the discriminator by producing images that are progressively more lifelike. In the meantime, the discriminator undergoes training to enhance its capacity to distinguish between real images and synthetic ones, accommodating a range of application scenarios. The GAN is trained using the loss function represented via equation 3,

$$minGmaxDV(D,G) = Ex \sim pdata(x)[logD(x)] + Ez \sim pz(z)\left[log\left(1 - D\left(G(z)\right)\right)\right] \quad (3)$$

Where, Ex~pdata(x)[logD(x)] is the expectation of the Discriminator's predictions on real data being recognized as real, while Ez~pz(z)[log(1-D(G(z)))] is the expectation of the Discriminator's predictions on fake data (generated by G) being recognized as fake. In this work, the GAN preprocesses MRI images by enhancing their quality, and clarity, and potentially highlighting critical features relevant to tumor detection. This preprocessing step ensures that the CNN, LSTM and BiGRU components of the BTLBD model receive input data of enhanced quality, Consequently, the overall efficacy of the tumor-detecting mechanism is increased. Thus, the GAN's role in preprocessing MRI images is crucial in the BTLBD model. Generating high-quality, enhanced images, lay a robust foundation for the subsequent sophisticated deep learning processes,

thereby augmenting the model's accuracy and reliability in the brain tumor detection process[32].

3.3 Segmentation

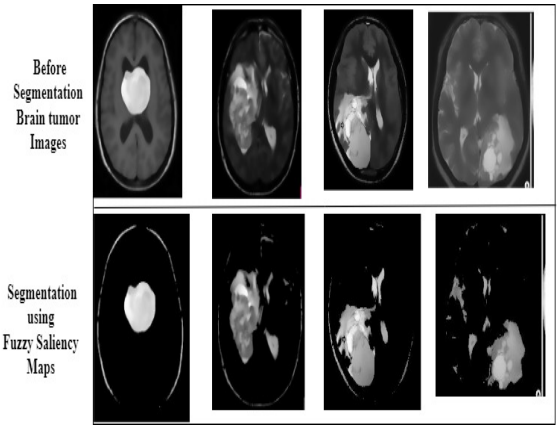

Figure. 4 Segmentation using Fuzzy saliency maps.

In Figure 4, These pre-processed images are segmented using Fuzzy Saliency Maps. This segmentation step is pivotal in isolating the region of interest – specifically, the brain tumor – from the rest of the brain tissue in the MRI images for different tumor types. The images, enhanced by the GAN, serve as the input to the Fuzzy Saliency Map model. The core of the Fuzzy Saliency Map model is a Fuzzy Inference System (FIS), which applies fuzzy logic principles to determine the saliency of each pixel in the MRI images & samples. The FIS consists of a set of fuzzy rules and membership functions that evaluate the pixel characteristics, such as intensity, contrast, and texture, to estimate their degree of belonging to a salient (tumor) region for different tumor types. The model uses an Intensity-Based Membership Function which is represented as μintensity(x), and evaluates the pixel intensity and assigns a membership value indicating its likelihood of being part of a tumor via equation 4,

$$\mu intensity(x) = exp(-\frac{(x-\mu t)^2}{2\sigma t^2}) \ldots (4)$$

Where x is the intensity value of a given pixel in the MRI image, μt is the mean intensity value that typically represents tumor regions in MRI scans. This value is determined based on the analysis of a training dataset & its samples. While σt ithe standard deviation of the intensity values within tumor regions, indicating the spread or variability of intensity values typically found in tumors. The function is essentially a Gaussian membership function, centered around μt, the mean intensity value for tumor regions. The exponent term calculates the squared difference between the pixel's intensity and the mean tumor intensity, normalized by the variance levels. The exponential function ensures that the membership value decreases as the pixel intensity deviates from the mean tumor intensity, with a steeper decrease for larger variances in the image sets. This function assigns higher membership values to pixels whose intensities are close to μt, indicating a higher likelihood of being part of a tumor for different input image sets. This function is used to evaluate each pixel in the pre-processed MRI images & samples. Pixels with higher membership values are more likely to be part of a tumor, guiding the model's focus toward potential tumor regions during the segmentation process. This function is integral to the fuzzy logic-based approach in the BTLBD model, contributing to the model's ability to accurately identify and segment tumor regions from the brain MRI scans.

Similarly, the model uses an efficient Texture-Based Membership Function represented as μtexture(x), this function assesses the texture around each pixel, crucial for distinguishing tumor tissues via equation 5,

$$\mu texture(x) = \frac{1}{1 + exp\left(-k \cdot (T(x) - Tthreshold)\right)} \ldots (5)$$

Where, x is the pixel under evaluation in the MRI image, T(x) represents a texture descriptor at pixel x which is derived from Local Binary Patterns (LBP), and Threshold is the texture threshold, distinguishing normal tissue from tumor tissue. This value is determined based on the analysis of training data, where the typical texture of tumor regions is studied for different image sets. While k is a scaling factor that adjusts the steepness of the membership function. T(x) calculates a texture measure at pixel x, reflecting the local texture patterns; T threshold acts as a reference point, differentiating between typical tumor textures and normal brain tissue textures. The function is a sigmoid function centered around the Threshold, and it yields a higher membership value for textures that are more characteristic of tumor tissues. The scaling factor k controls how rapidly the membership value changes concerning the difference between T(x) and Threshold levels. In the BTLBD model, μtexture(x) is utilized to evaluate the texture around each pixel in the pre-processed MRI images & samples. Pixels with

higher membership values are indicative of textures that are more characteristic of tumor tissues. This texture-based analysis complements the intensity-based assessment, providing a more comprehensive approach to identifying and segmenting tumor regions in brain MRI scans. The integration of this function into the model's segmentation process enhances its ability to accurately differentiate between tumor and non-tumor tissues, contributing to the overall efficacy of the BTLBD model in the brain tumor detection process.

The fuzzy logic rules combine the membership values from different functions to create a comprehensive saliency map from input image sets. This aggregation is performed using fuzzy operators. The output is a saliency value for each pixel, indicating its probability of being part of the tumor region. The aggregated fuzzy saliency values are then converted into real values to form a clear, segmented image indicating for different tumor types. This process, known as defuzzification, involves the max-membership principles. The result is a segmented MRI image where the tumor regions are distinctly isolated from the non-tumor areas.

The Fuzzy Saliency Map model is integral in accurately segmenting brain tumors from MRI images & samples. This segmentation is critical for the subsequent phases of the BTLBD model, where precise detection and classification of tumors are performed. By employing fuzzy logic, the model adeptly handles the inherent uncertainties and variations in medical images, ensuring a robust and accurate segmentation process. This model serves as an essential bridge between the preprocessing and classification stages of the BTLBD model. Its ability to accurately segment tumor regions, significantly improves the model's overall performance, ensuring that the subsequent LSTM, BiGRU, and CNN components operate on accurately isolated tumor regions, leading to more precise brain tumor detection and classification [33].

3.4 Feature Extraction:

Principal component analysis (PCA) is a statistical method for dimensionality reduction, feature extraction, and data visualization. It converts high-dimensional data into a lower-dimensional space while retaining maximal variance (information).

When applying Principal Component Analysis (PCA) for feature extraction from brain tumor MRI segmented images, the mathematical framework involves several steps, as detailed below:

1.Organize Data into Matrix: let X represent the dataset of MRI segmented image .Each image is vectorized into a 1D array ,resulting in a data matrix:

$$X= \begin{bmatrix} x1,1 & x1,2\cdots & x1,n \\ x2,1 & x2,2\ldots & x2,n \\ xm,1 & xm,2\cdots & xm,n \end{bmatrix}$$

m:number of images (dampless)

n:Number of pixels(features per images.

2.Standardize the Data:

Subtract the mean of each feature (pixel intensity across images) to center the data

Hear ,$\bar{X}$ is the mean – cantered matrix.

3.Compute the covariance Matrix:

Calculate the covariance matrix to understand the relationships between feature:

$$C = \frac{1}{m-1}\bar{X}^T\bar{X}$$

Where C is the nxm matrix.

III. Eigenvalue Decomposition :

Compute the eigenvalue represents(λ)and eigenvector () of the covariance matrix C:

$$C\vartheta = \lambda\vartheta$$

The eigenvalue represents the principal components. The eigenvalue quantity the amount of variance captured by each principal component.

5.Sort and Select Principal Components:

Sort eignenvalues $\lambda_1, \lambda_2, \ldots\ldots\ldots\ldots \lambda_n$in descending order and select the top k eigenvectors V_k :

$$\bar{X}_{ij} = X_{ij} - \mu_j, \mu_j = \frac{1}{m}\sum_{i=1}^{m} X_{ij}$$

Vk=[υ_(1,) υ_(2,)……..,υ_(k,)

6.project Data onto Principal Components:

Transform the original data to the new k-dimensions space :

Z=X¯V_k

3.5 Feature Selection

Horse herd optimization algorithm

1. Population initialization

The position of N horses in a D- dimensional search space is initialized as follows

$X_i=[x_{i1}, x_{i2},\ldots,x_{iD}]$, for i=1,2,……..,N

The positions are randomly initialized within predefined search bounds: Xij€$[x_{min}, x_{max}]$.

2. The best horse (Leader) guides the exploration phase.

the leader position X_{best} is determined based on fitness and the position of the horse is updated using.

$$X_i^{t+1} = X_{best}^{f} + r1.\left(X_{best}^{t} - X_i^{t}\right)$$

The equation encourages the horses to move toward the leader with some randomness to ensure exploration.

3.Herd Following Behavior (Exploitation Phase)

Horses follow the leader but also interact with other horses to enhanced local search:

$$X_i^{t+1} = X_i^{t} + r2.\left(X_{best}^{t} - X_i^{t}\right) + r3.\left(X_k^{t} - X_i^{t}\right)$$

The second term moves the horse toward the leader, while the third term models the interaction with a randomly chosen horse for local exploitation.

4.Social Learning (Combination of Exploration and Exploitation)

To balance Exploration and exploitation, the horse also learns from both the leader and other head members. the position update is given by

$$X_i^{t+1} = X_i^{t} + r_4.(X_{best}^{t} - X_i^{t} + r5.\left(\sum_{j=1}^{N} X_j^{t} - X_i^{t}\right.$$

This equation models a combination of the influence of the leader and the collective behaviour of the herd.

5.Boundary that horses stay with in search space boundaries, their positions, are adjusted as follows.

$X_{ij}=\{X_{min}$ if $X_{ij} < X_{min}$
X_{max} if $X_{ij} > X_{max}$
X_{ij} otherwise$\}$

Where X_{ij} is the position of the i th horse in the jth dimension.

6.Fitness Evaluation

At each iteration, the fitness of each horse X_i is evaluated using the objective function $f(X_i)$.the best horse X_{best} is updated as follows:

X_{best}=argmin $f(X_i), \forall i = 1,2,\ldots..,N$

7.Stopping Criteria

The algoritham stops when a predefined number of iteration T_{max} is reached .

3.6 Classification

These segmented images are given to an efficient feature extraction unit that uses a fusion of CNN, Long Short-Term Memory (LSTM) and Bidirectional Gated Recurrent Units (BiGRU). This combined method uses the best features of CNN, LSTM, and BiGRU architectures to quickly and accurately pull out temporal and spatial features from segmented MRI images, which is necessary for accurately classifying brain tumors. [34]. LSTM units consist of a cell state and three gates – forget, input, & output, gates, which are represented via equations 6, 7 & 8 respectively as follows,

$$ft = \sigma(Wf \cdot [ht-1, xt] + bf) \ldots (6)$$

$$it = \sigma(Wi \cdot [ht-1, xt] + bi) \ldots (7)$$

$$C\sim t = \boldsymbol{tanh}(WC \cdot [ht-1, xt] + bC) \ldots (8)$$

The final cell state is represented via equation 9,

$$Ct = ft * Ct - 1 + it * C\sim t \ldots (9)$$

While the output features are estimated via equation 10,

$$ot = \sigma(Wo \cdot [ht-1, xt] + bo) \ldots (10)$$

$$ht = ot * \boldsymbol{tanh}(Ct) \ldots (11)$$

In these estimations, W & b represent different weights & biases. Based on these evaluations, the LSTM Model Captures temporal dependencies within the image sequence, crucial for understanding the progression of brain tumors. Similarly, BiGRU consists of two GRUs processing the data in forward and reverse scopes. This is done using Update Gate, Reset Gate, Candidate Activation & Final Output operations, which are represented via equations 12, 13, 14 & 15 as follows,

$$zt = \sigma(Wz \cdot [ht-1, xt] + bz) \dots (12)$$

$$rt = \sigma(Wr \cdot [ht-1, xt] + br) \dots (13)$$

$$h\sim t = \boldsymbol{tanh}(W \cdot [rt * ht-1, xt] + b) \dots (14)$$

$$ht = (1-zt) * ht-1 + zt * h\sim t \dots (15)$$

IV. This procedure improves the model's capacity to grasp both historical and prospective context, yielding a thorough comprehension of spatial features in the images and samples. The outputs from LSTM and BiGRU are fused using a weighted process via equation 16,

$$Ft = \alpha \cdot HLSTM + (1-\alpha) \cdot HBiGRU \dots (16)$$

This operation combines the strengths of CNN, LSTM and BiGRU, ensuring a robust feature extraction process. The result of this fusion process is a collection of features that encapsulate the temporal progression and spatial context of the segmented brain tumors. The integrated CNN, LSTM and BiGRU architecture is instrumental in extracting detailed and nuanced features from segmented brain tumor images [35]. The LSTM component is adept at understanding the temporal evolution of the tumors, while the BiGRU provides a more comprehensive spatial analysis by considering both forward and backward context in the image sequence sets. The fusion of these two architectures ensures that the extracted features are both rich and representative of the complex nature of brain tumors, hence improving the accuracy and reliability of the subsequent classification stages. The combined CNN, LSTM and BiGRU model within the BTLBD framework represents a sophisticated approach to We are using feature extraction for the identification of brain tumors. By efficiently processing segmented MRI images and extracting critical features, this model significantly contributes to The correct categorization of brain tumors, marking a notable advancement in medical imaging and diagnostics [36].

These features are further processed for classification using a Convolutional Neural Network (CNN) process described in Figure 5. The CNN is specifically designed to handle the sequential nature of the input features, making it well suited for classifying The intricate patterns associated with brain tumors are fascinating. As its input, the convolutional neural network (CNN) uses the features extracted from the LSTM and BiGRU fusion, which encapsulate both temporal and spatial characteristics of the brain tumors [37]. The CNN consists of several convolutional layers, each aimed at extracting more advanced features from the input datasets via equation 17,

$$Fout = ReLU(W * Fin + b) \dots (17)$$

The convolution operation (W∗Fin) applies filter W to the input features Fin, followed by an addition of bias b and the application of a ReLU activation process. For this work, the configurations include 32, 64, and 128 filters in consecutive layers, with kernel sizes ranging from 3 to 5 for individual layers. After this, the Pooling layers (max pooling) follow convolutional layers to reduce the dimensionality of the feature maps, thus reducing computational complexity and overfitting operations. To prepare it for input into the fully linked layers, the last pooling layer transforms its output into a one-dimensional vector. After this, one or more fully connected layers follow the flattening process. These layers integrate the learned features for the final classification via equation 18,

$$Fdense = ReLU(Wdense \cdot Fflat + bdense) \dots (18)$$

V. The final layer is a SoftMax layer that outputs the probability distribution over the brain tumor classes via equation 19,

$$P(class \mid input) = Softmax(Woutput \cdot Fdense + boutput)$$

The learned features categorize the input MRI image into a specific brain tumor class. The BTDBD in this model is essential for the ultimate classification of brain tumors. Once the LSTM and BiGRU layers have successfully extracted and integrated the pertinent features from the MRI images, the CNN takes over to conduct a more detailed analysis. Through its convolutional and pooling layers, CNN can discern intricate patterns and relationships within the features, essential for

accurate tumor classification. The use of Softmax activation functions ensures non-linearity in the model, allowing it to capture complex dependencies.

The Softmax layer at the end maps the final feature representations to the probability distribution over the tumor classes, facilitating precise classification operations. This CNN model within the BTLBD framework is integral to the accurate and reliable classification of brain tumors. Its sophisticated layer structure and specialized configuration for processing the LSTM and BiGRU extracted features make it a powerful tool in the BTLBD model, ultimately contributing to enhanced diagnostic capabilities in the realm of medical imaging scenarios. In the subsequent section of this work, we evaluate the efficacy of this model using various metrics and compare it with existing methods [38].

The Brain Tumor Location and Boundary Detection (BTLBD) model represents a pioneering advancement in the field of medical imaging and diagnostics. Integrating the sophisticated methodologies of Convolutional Neural Network (CNN) architectures, Long Short-Term Memory

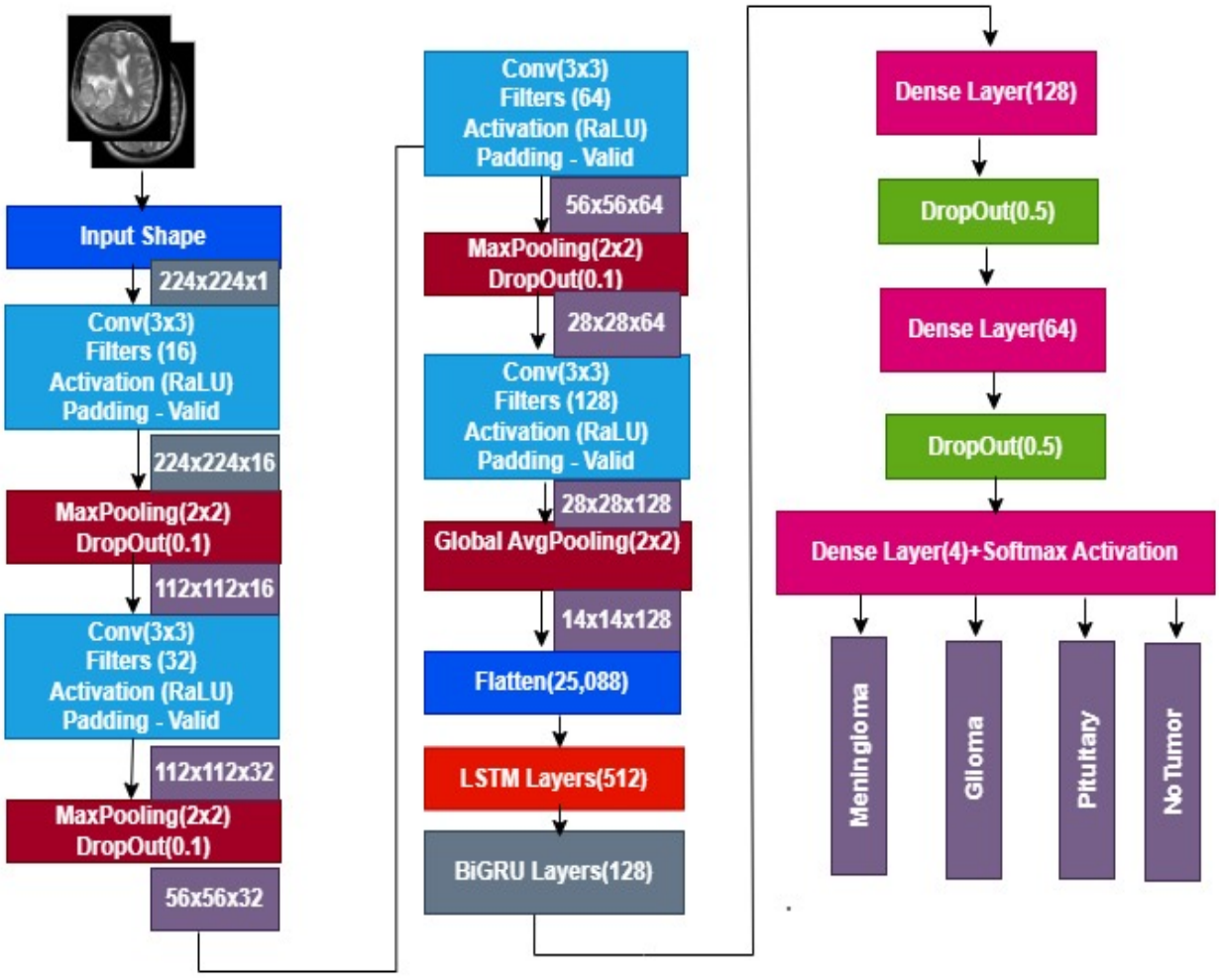

Figure 5. Architecture of the CNN, LSTM, BiGRU Process

(LSTM) and Bidirectional Gated Recurrent Units (BiGRU), the BTLBD model is meticulously designed to address the intricacies involved in brain tumor detection. Its unique fusion of CNN, LSTM and BiGRU allows for capturing both temporal dependencies and spatial features within brain imaging data, enhancing the model's ability to accurately identify and classify various brain

tumor types. The incorporation of CNN further refines the feature extraction process, allowing for a more nuanced and detailed analysis of the MRI scans. This combination enhances the model's precision and accuracy while ensuring rapid processing, a crucial element in clinical environments. By delivering high performance across key metrics such as precision, accuracy, recall, and specificity, The BTLBD model establishes a new standard in medical diagnostics, providing a substantial advancement in the early and accurate identification of brain cancers.

Architecture: The BTLBD model combined CNN, LSTM and BiGRU layers. The LSTM and BiGRU layers were configured with 128 units each, while the CNN component comprised convolutional layers with filter sizes of 32, 64, and 128 Model Configuration. Activation Functions: ReLU was used for intermediate layers, while a Softmax activation function was employed in the output layer for multiclass classification.

4.Result Analysis

In this study, Table 2 presents the details of the Brain Tumor MRI dataset, outlining the splits for training, testing, and validation purposes. Kaggle Brain tumor MRI datasets are used The Training dataset has a total of samples, out of which 1339 samples correspond to Meningioma,1321 Glioma samples,1457 Pituitary samples, and 1595 No tumor samples.

The Testing dataset contains a total sample from which 306 Meningioma samples, 300 Glioma samples, 300 Pituitary samples, and 405 No tumor samples. The MRI brain tumor dataset is openly accessible research community for academic purposes. To combine both Training and testing data sets,1645 Meningioma Images, 1621 Glioma Images, 1757 pituitary Images, and 2000 No Tumor images. The total Images is 7023. The data are separated into training 70% (4916 pictures), testing 15% (1053 images), and validation 15 %(1053 images).

In table 3: The total Images is 21069. The data are separated into training 70% (14751 pictures), testing 15% (3159 images), and validation 15 %(3159 images).

TABLE 2. Brain Tumor MRI Dataset for Using Splitting Training and Testing with out Augmentation

Classification	Training Images (70%)	Testing Images (15%)	Validation Images (15%)	Total
Meningioma	1151	247	247	1645
Glioma	1135	243	243	1621
Pituitary	1231	263	263	1757
No tumor	1400	300	300	2000
Total	4917	1053	1053	7023

TABLE 3. Brain Tumor MRI Dataset for Using Splitting Training and Testing with Augmentation

Classification	Training Images (70%)	Testing Images (15%)	Validation Images (15%)	Total
Meningioma	3453	741	741	4935
Glioma	3405	729	729	4863
Pituitary	3693	789	789	5271
No tumor	4200	900	900	6000
Total	14751	3159	3159	21069

Table 4. BTLBD Model Training Hyper Parameres.

SNO	Parameter used	Value
1	Training Epochs	100
2	Optimizer	Adam
3	Learning Rate	0.0001
4	Batch size	32
5	Loss Function	Categorical Cross Entropy

Table 4: presents the hyperparameters used for training the BTLBD model, including the optimizer, batch size, loss function, learning rate, and activation functions.

The BTLBD model's performance was benchmarked against existing models like LCDEiT, RU-Net2+, and ResUNet+. This comparative analysis was vital in establishing the superiority of the BTLBD model in terms of the aforementioned metrics.

$$Precision = \frac{TP}{TP + FP} \dots (20)$$

$$Accuracy = \frac{TP + TN}{TP + TN + FP + FN} \dots (21)$$

$$Recall = \frac{TP}{TP + FN} \dots (22)$$

$$AUC = \int TPR(FPR)dFPR \dots (23)$$

$$Sp = \frac{TN}{TN + FP} \dots (24)$$

$$D = ts(complete) - ts(init) \dots (25)$$

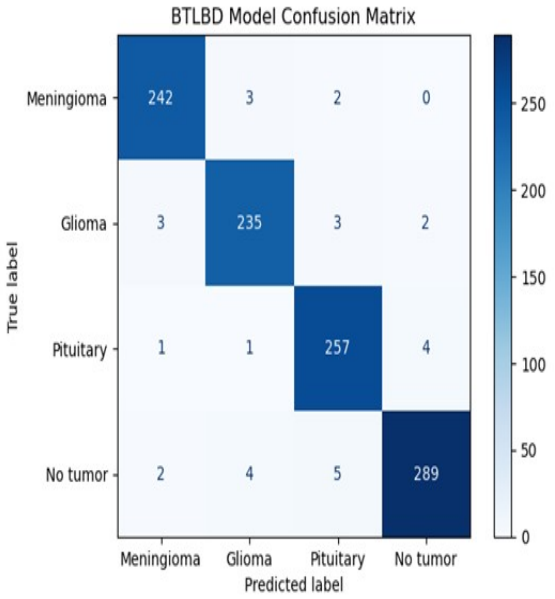

Figure. 6. Confusion Matrix of BTLBD Model With Out Augmentation

Figure 6: presents the confusion matrix for the BTLBD model, The model's effectiveness is demonstrated by displaying the distribution of correct and incorrect classifications across all classes. Rows represent the true labels. Columns represent the predicted labels. The diagonal elements denote the quantity of accurate forecasts for each class. Off-diagonal elements denote misclassifications. i.e., where the model predicted the wrong class. Figure 7 presents the confusion matrix of the BTLBD model with data augmentation applied, illustrating the model's classification performance across different classes.

Journal of Theoretical and Applied Information Technology
28th February 2025. Vol.103. No.4

ISSN: 1992-8645 www.jatit.org E-ISSN: 1817-3195

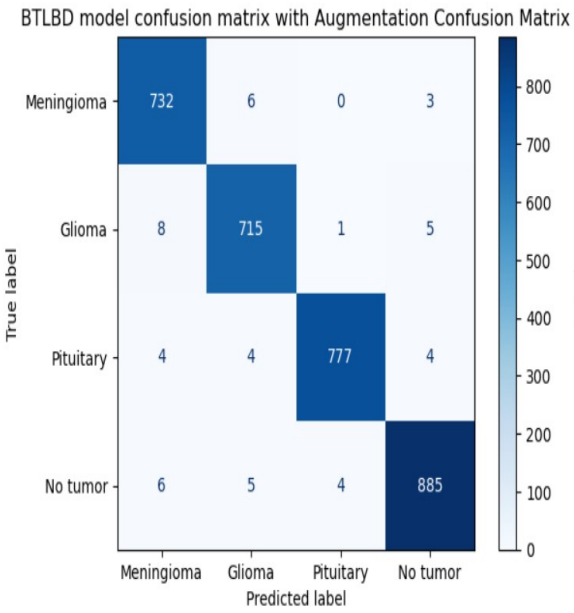

Figure . 7. Confusion Matrix of BTLBD Model with Augmentation

Figure 8 demonstrates the classification performance of the BTLBD model across four distinct classes: meningioma, glioma, pituitary, and no tumor. The evaluation metrics shown in the figure include precision, recall, and F1-score, which are fundamental measures used to assess the effectiveness of the model in detecting each class.

When applying data augmentation techniques, Figure 9 displays the performance metrics Precision, Recall, and F1-score for the BTLBD model. The classes evaluated remain consistent with the previous analysis, including meningioma, glioma, pituitary, and no tumor. We evaluate each class using three primary metrics: precision (blue), recall (green), and F1-score (red).

Table 5 presents the precision, recall, and F1-score values for the BTLBD model and the BTLBD model with augmentation. The findings illustrate the relative efficacy of both strategies across all classes: meningioma, glioma, pituitary, and no tumor. The inclusion of data augmentation improves the model's robustness, as indicated by the high and consistent values for all performance metrics across both configurations.

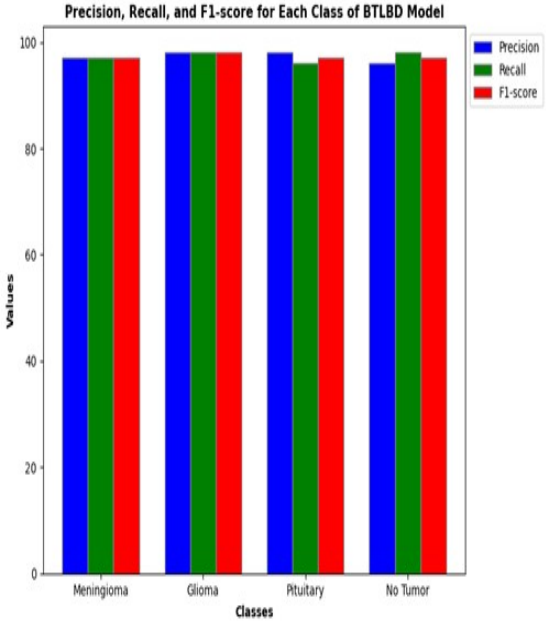

Figure 8. Shows Confusion matrix values of the BTLBD Model without Augmentation.

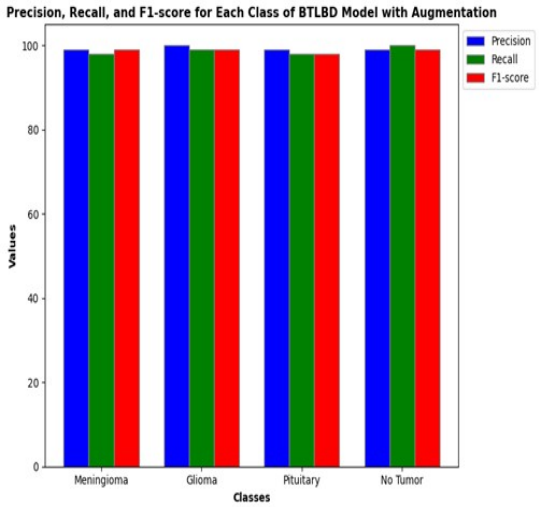

Figure 9. Shows Confusion matrix values of the BTLBD Model with Augmentation.

Table 5. precision, Recall, F1-Scope Values of BTLBD Model, BTLBD Model with Augmentation.

Model	class	precision %	recall %	f1-score %
BTLBD Model without Augmentation.	meningioma	96	97	97
	glioma	98	97	96
	pituitary	98	96	97
	No tumor	96	98	97
BTLBD Model with Augmentation.	meningioma	99	98	99
	glioma	100	99	99
	pituitary	99	100	98
	No tumor	99	100	99

Figure 10 illustrates the variation in accuracy of the BTLBD model across different training epochs, comparing performance with and without data augmentation. The x-axis represents the number of epochs (25, 50, 75, and 100), while the y-axis denotes the model's accuracy in percentage.

Without Augmentation (blue bars): The model's accuracy steadily improves with increased training epochs, starting at 96.12% at 25 epochs and rising to 97.19% at 100 epochs. This shows that as the number of epochs increases, the model becomes better at learning from the data.

With Augmentation (orange bars): The accuracy consistently outperforms the non-augmented model at every epoch, starting at 97.24% at 25 epochs and increasing to 98.95% at 100 epochs. The use of augmentation enhances the model's ability to generalize better, likely due to the increased variability in the training data.

Figure 11 illustrates the Training and Validation Accuracy Graph and the Training and Validation Loss Graph for the BTLBD model. These graphs provide a visual representation of the model's performance during training, showing how accuracy improves and loss decreases over time for both training and validation datasets.

Figure 12 shows These graphs display the accuracy and loss results from both training and validation for the BTLBD model with augmentation. These graphs illustrate the model's performance over the training process, highlighting the improvements in accuracy and reductions in loss when data augmentation is applied.

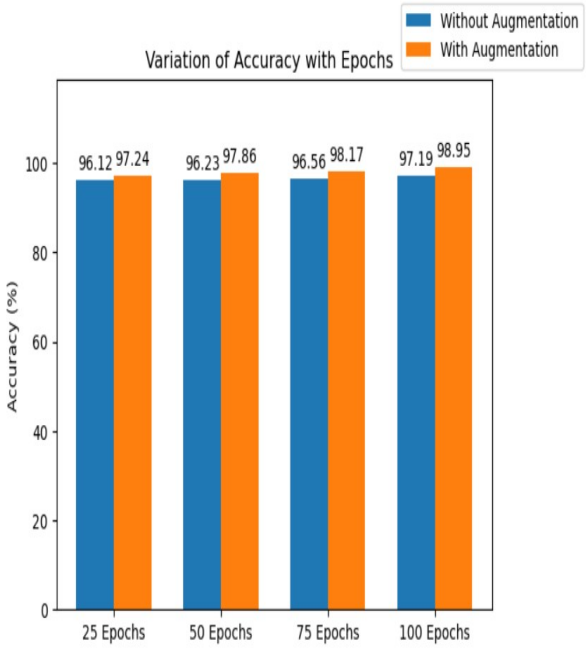

Figure. 10. Variation of Accuracy with Different Epochs BTLBD MODEL.

Table 6 compares the accuracy of the proposed BTLBD model (with and without augmentation) with other state-of-the-art models in the literature. The proposed BTLBD model achieves an accuracy of 97.19% without augmentation and 98.95% with augmentation, which demonstrates a significant performance improvement when augmentation is applied. Notably, the proposed model outperforms several other methods, such as LCDEiT (93.69%), ResUNet+ (93.10%), and shows competitive results compared to RU-Net2+ (98.51%).

Figure 13 shows Comparison of Exiting Models Accuracy and proposed models Accuracy. The accuracy of various models is compared on the test set. The models include LCDEiT[5], ResUNet+[29], RU-Net2+[15], BTLBD Model and BTLBD Model with Augmentation. The BTLBD model .

Journal of Theoretical and Applied Information Technology
28th February 2025. Vol.103. No.4

ISSN: 1992-8645 www.jatit.org E-ISSN: 1817-3195

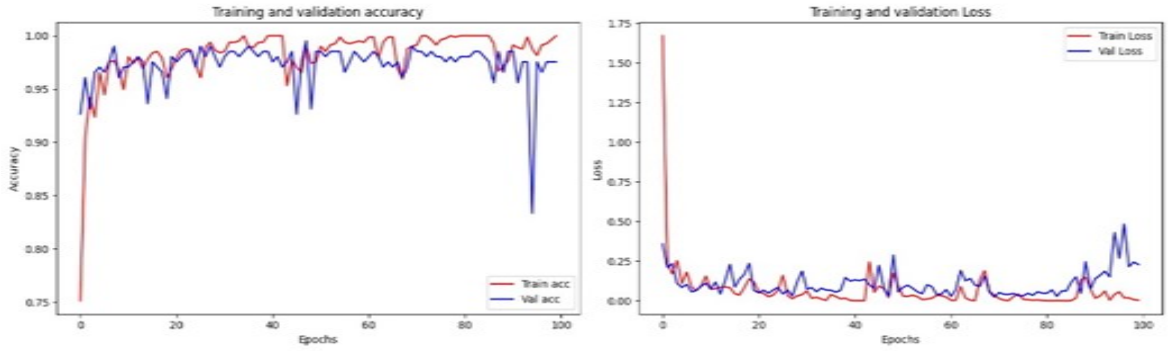

Figure 11. The Training && Validation Accuracy Graph And Training && Validation Loss Graph Of The BTLBD Model

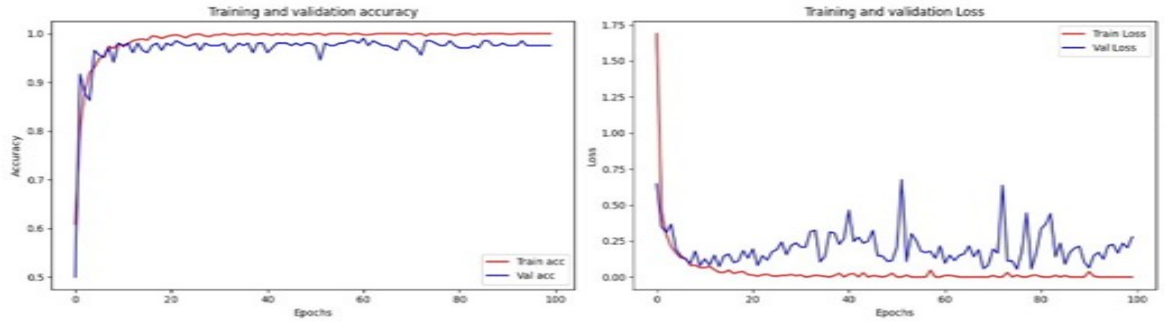

Figure 12. These Graphs Display The Accuracy And Loss Results From Both Training And Validation Of The BTLBD Model With Augmentation.

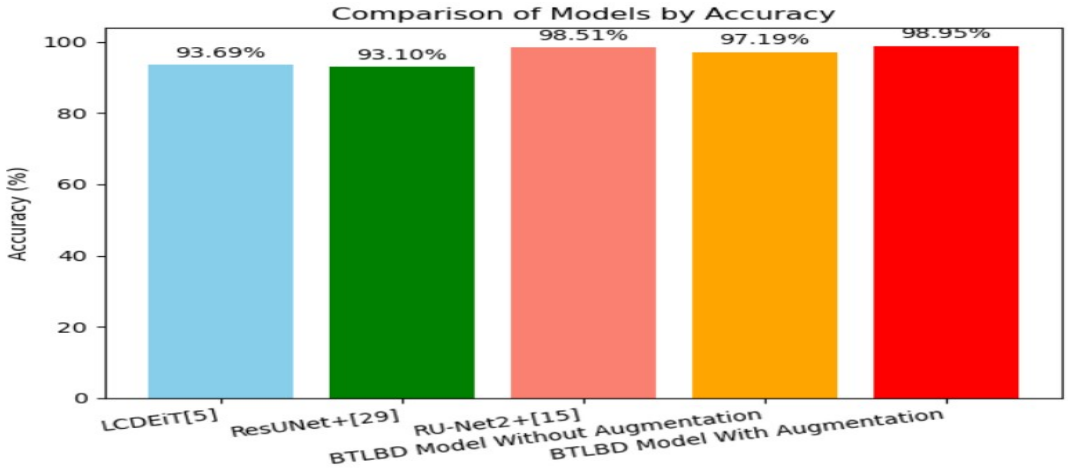

Figure. 13. Comparison Of Exiting Models Accuracy And Proposed Models Accuracy.

Table 6: Accuracy Comparison Of Various Methods.

Sno	Author	Accuracy
1	LCDEiT[5]	93.69%
2	ResUNet+[29]	93.10%
3	RU-Net2+[15]	98.51%

4	**Proposed BTLBD Model Without Augmentation.** **BTLBD-Model WithAugmentation**	**97.19%** **98.95%**

5.CONCLUSION

this work addresses critical gaps in the diagnosis of brain tumors by introducing a robust and innovative deep learning model. For example, GANs are used to make the data better, the CNMF filter lowers the noise, fuzzy saliency maps separate the data into groups, and HHO selects the best features to ensure the classification is correct. The integration of CNN, LSTM, and BiGAN models further enhances the model's ability to classify brain tumor types accurately. The proposed method is much better than the current one; it can make diagnoses 97.19% of the time without augmentation and 98.95% of the time with augmentation.

This work is a significant step towards connecting deep learning with practical medical applications. Combining different architectures and optimization methods makes tumor detection more reliable, which could lead to earlier diagnoses and better patient outcomes.

The integration of multiple deep learning models significantly improves accuracy and reliability in tumor detection. The use of CNMF for noise reduction and GANs for data augmentation enhances image quality and dataset diversity.

The implications of this research extend beyond the immediate application of brain tumor diagnoses. By streamlining and improving diagnostic accuracy, the model has the potential to facilitate timely interventions, improve patient outcomes, and reduce the associated emotional and financial strain on healthcare systems. Furthermore, this methodology lays a foundation for broader applications in medical imaging, setting a new benchmark in leveraging deep learning for complex diagnostic challenges. Ultimately, this work serves as a meaningful step forward in the integration of artificial intelligence in healthcare, contributing to more precise, efficient, and accessible medical diagnostics. The clinical impacts of the BTLBD model are far-reaching. Its ability to accurately and quickly diagnose brain tumors holds significant implications for patient care. Timely and accurate identification of brain tumors might result in enhanced treatment strategizing, thereby enhancing patient prognosis. The reduction in diagnostic delay can be particularly beneficial in acute care settings, while the high specificity and precision can decrease the emotional and financial burden on patients due to unnecessary treatments or procedures.

To summarize, The BTLBD model represents a significant advancement in the integration of deep learning and medical diagnostics. Utilizing this technology for brain tumor identification improves both precision and speed of diagnosis, as well as the potential to improve patient outcomes and optimize healthcare procedures. This discovery not only provides a significant addition to the field of medical image processing but also expands the potential for broader applications of artificial intelligence in healthcare. This research promises to perform complex diagnostic tasks with greater accuracy, efficiency, and a focus on patient well-being in the future. In feature work, we are looking into more advanced generative models, like diffusion models and transformers, to improve the production of synthetic data and successfully add to smaller datasets. We are investigating alternative or hybrid optimization methods beyond Horse Head Optimization (HHO), including Particle Swarm Optimization (PSO) and Differential Evolution, to improve feature selection.

LIMITATIONS

A limitation of this work is that it requires an increase in the number of images in the dataset to further improve the model's generalizability and performance." It might be worth looking into more advanced GAN architectures, like StyleGAN, Progressive GAN, or Diffusion Models, to make synthetic images that look more real and varied. This would cut down on any possible biases and make it easier to classify different types of tumors.

ACKNOWLEDGMENT

The authors to express their gratitude to VIT-AP University for its support and provision of resources that facilitated the execution of this research.

Conflicts of Interest: ‘‘The authors declare no conflict of interest.’’

REFERENCES

[1] H. A. Shah, F. Saeed, S. Yun, J. -H. Park, A. Paul and J. -M. Kang, "A Robust Approach for Brain Tumor Detection in Magnetic Resonance Images Using Finetuned EfficientNet," in IEEE Access, vol. 10, pp. 65426-65438, 2022, doi: 10.1109/ACCESS.2022.3184113.

[2] I. Ezhov et al., "Geometry-Aware Neural Solver for Fast Bayesian Calibration of Brain Tumor Models," in IEEE Transactions on Medical Imaging, vol. 41, no. 5, pp. 1269-1278, May 2022, doi: 10.1109/TMI.2021.3136582.

[3] S. Ahmad and P. K. Choudhury, "On the Performance of Deep Transfer Learning Networks for Brain Tumor Detection Using MR Images," in IEEE Access, vol. 10, pp. 59099-59114, 2022, doi: 10.1109/ACCESS.2022.3179376.

[4] A. Kujur, Z. Raza, A. A. Khan and C. Wechtaisong, "Data Complexity Based Evaluation of the Model Dependence of Brain MRI Images for Classification of Brain Tumor and Alzheimer's Disease," in IEEE Access, vol. 10, pp. 112117-112133, 2022, doi: 10.1109/ACCESS.2022.3216393.

[5] G. J. Ferdous, K. A. Sathi, M. A. Hossain, M. M. Hoque and M. A. A. Dewan, "LCDEiT: A Linear Complexity Data-Efficient Image Transformer for MRI Brain Tumor Classification," in IEEE Access, vol. 11, pp. 20337-20350, 2023, doi: 10.1109/ACCESS.2023.3244228.

[6] M. Rahimpour et al., "Cross-Modal Distillation to Improve MRI-Based Brain Tumor Segmentation With Missing MRI Sequences," in IEEE Transactions on Biomedical Engineering, vol. 69, no. 7, pp. 2153-2164, July 2022, doi: 10.1109/TBME.2021.3137561.

[7] A. Bs, A. V. Gk, S. Rao, M. Beniwal and H. J. Pandya, "Electrical Phenotyping of Human Brain Tissues: An Automated System for Tumor Delineation," in IEEE Access, vol. 10, pp. 17908-17919, 2022, doi: 10.1109/ACCESS.2022.3149803.

[8] S. Mohsen, A. M. Ali, E. -S. M. El-Rabaie, A. ElKaseer, S. G. Scholz and A. M. A. Hassan, "Brain Tumor Classification Using Hybrid Single Image Super-Resolution Technique With ResNext101_32× 8d and VGG19 Pre-Trained Models," in IEEE Access, vol. 11, pp. 55582-55595, 2023, doi: 10.1109/ACCESS.2023.3281529.

[9] M. Renugadevi et al., "Machine Learning Empowered Brain Tumor Segmentation and Grading Model for Lifetime Prediction," in IEEE Access, vol. 11, pp. 120868-120880, 2023, doi: 10.1109/ACCESS.2023.3326841.

[10] Y. Zhuang, H. Liu, E. Song and C. -C. Hung, "A 3D Cross-Modality Feature Interaction Network With Volumetric Feature Alignment for Brain Tumor and Tissue Segmentation," in IEEE Journal of Biomedical and Health Informatics, vol. 27, no. 1, pp. 75-86, Jan. 2023, doi: 10.1109/JBHI.2022.3214999.

[11] A. BS, A. B, H. RS, V. V, A. Mahadevan and H. J. Pandya, "Electromechanical Characterization of Human Brain Tissues: A Potential Biomarker for Tumor Delineation," in IEEE Transactions on Biomedical Engineering, vol. 69, no. 11, pp. 3484-3493, Nov. 2022, doi: 10.1109/TBME.2022.3171287.

[12] J. Lin et al., "CKD-TransBTS: Clinical Knowledge-Driven Hybrid Transformer With Modality-Correlated Cross-Attention for Brain Tumor Segmentation," in IEEE Transactions on Medical Imaging, vol. 42, no. 8, pp. 2451-2461, Aug. 2023, doi: 10.1109/TMI.2023.3250474.

[13] S. Subramanian, A. Ghafouri, K. M. Scheufele, N. Himthani, C. Davatzikos and G. Biros, "Ensemble Inversion for Brain Tumor Growth Models With Mass Effect," in IEEE Transactions on Medical Imaging, vol. 42, no. 4, pp. 982-995, April 2023, doi: 10.1109/TMI.2022.3221913.

[14] B. Cheng, C. Bing, T. H. Chu, S. Alzahrani, S. Pichardo and G. B. Pike, "Simultaneous Localized Brain Mild Hyperthermia and Blood-Brain Barrier Opening via Feedback-Controlled Transcranial MR-Guided Focused Ultrasound and Microbubbles," in IEEE Transactions on Biomedical Engineering, vol. 69, no. 6, pp. 1880-1888, June 2022, doi: 10.1109/TBME.2021.3130164.

[15] R. Zaitoon and H. Syed, "RU-Net2+: A Deep Learning Algorithm for Accurate Brain Tumor Segmentation and Survival Rate Prediction," in IEEE Access, vol. 11, pp. 118105-118123, 2023, doi: 10.1109/ACCESS.2023.3325294.

[16] J. Zhao et al., "Uncertainty-Aware Multi-Dimensional Mutual Learning for Brain and Brain Tumor Segmentation," in IEEE Journal of Biomedical and Health Informatics, vol. 27, no. 9, pp. 4362-4372, Sept. 2023, doi: 10.1109/JBHI.2023.3274255.

[17] M. A. Ottom, H. A. Rahman and I. D. Dinov, "Znet: Deep Learning Approach for 2D MRI Brain Tumor Segmentation," in IEEE Journal of Translational Engineering in Health and Medicine, vol. 10, pp. 1-8, 2022, Art no. 1800508, doi: 10.1109/JTEHM.2022.3176737.

[18] M. V. S. Ramprasad, M. Z. U. Rahman and

M. D. Bayleyegn, "SBTC-Net: Secured Brain Tumor Segmentation and Classification Using Black Widow With Genetic Optimization in IoMT," in IEEE Access, vol. 11, pp. 88193-88208, 2023, doi: 10.1109/ACCESS.2023.3304343.

[19] Y. Ding et al., "MVFusFra: A Multi-View Dynamic Fusion Framework for Multimodal Brain Tumor Segmentation," in IEEE Journal of Biomedical and Health Informatics, vol. 26, no. 4, pp. 1570-1581, April 2022, doi: 10.1109/JBHI.2021.3122328.

[20] A. Sekhar, S. Biswas, R. Hazra, A. K. Sunaniya, A. Mukherjee and L. Yang, "Brain Tumor Classification Using Fine-Tuned GoogLeNet Features and Machine Learning Algorithms: IoMT Enabled CAD System," in IEEE Journal of Biomedical and Health Informatics, vol. 26, no. 3, pp. 983-991, March 2022, doi: 10.1109/JBHI.2021.3100758.

[21] C. Chen et al., "Synthesizing MR Image Contrast Enhancement Using 3D High-Resolution ConvNets," in IEEE Transactions on Biomedical Engineering, vol. 70, no. 2, pp. 401-412, Feb. 2023, doi: 10.1109/TBME.2022.3192309.

[22] S. Solanki, U. P. Singh, S. S. Chouhan and S. Jain, "Brain Tumor Detection and Classification Using Intelligence Techniques: An Overview," in IEEE Access, vol. 11, pp. 12870-12886, 2023, doi: 10.1109/ACCESS.2023.3242666.

[23] S. Alagarsamy, V. Govindaraj and S. A, "Automated Brain Tumor Segmentation for MR Brain Images Using Artificial Bee Colony Combined With Interval Type-II Fuzzy Technique," in IEEE Transactions on Industrial Informatics, vol. 19, no. 11, pp. 11150-11159, Nov. 2023, doi: 10.1109/TII.2023.3244344.

[24] C. Yan, J. Ding, H. Zhang, K. Tong, B. Hua and S. Shi, "SEResU-Net for Multimodal Brain Tumor Segmentation," in IEEE Access, vol. 10, pp. 117033-117044, 2022, doi: 10.1109/ACCESS.2022.3214309.

[25] A. Jabbar, S. Naseem, T. Mahmood, T. Saba, F. S. Alamri and A. Rehman, "Brain Tumor Detection and Multi-Grade Segmentation Through Hybrid Caps-VGGNet Model," in IEEE Access, vol. 11, pp. 72518-72536, 2023, doi: 10.1109/ACCESS.2023.3289224.

[26] H. Yang, T. Zhou, Y. Zhou, Y. Zhang and H. Fu, "Flexible Fusion Network for Multi-Modal Brain Tumor Segmentation," in IEEE Journal of Biomedical and Health Informatics, vol. 27, no. 7, pp. 3349-3359, July 2023, doi: 10.1109/JBHI.2023.3271808.

[27] S. Rajendran et al., "Automated Segmentation of Brain Tumor MRI Images Using Deep Learning," in IEEE Access, vol. 11, pp. 64758-64768, 2023, doi: 10.1109/ACCESS.2023.3288017.

[28] M. Ismail et al., "Radiomic Deformation and Textural Heterogeneity (R-DepTH) Descriptor to Characterize Tumor Field Effect: Application to Survival Prediction in Glioblastoma," in IEEE Transactions on Medical Imaging, vol. 41, no. 7, pp. 1764-1777, July 2022, doi: 10.1109/TMI.2022.3148780.

[29] S. Metlek and H. Çetıner, "ResUNet+: A New Convolutional and Attention Block-Based Approach for Brain Tumor Segmentation," in IEEE Access, vol. 11, pp. 69884-69902, 2023, doi: 10.1109/ACCESS.2023.3294179.

[30] A. Farzamnia, S. H. Hazaveh, S. S. Siadat and E. G. Moung, "MRI Brain Tumor Detection Methods Using Contourlet Transform Based on Time Adaptive Self-Organizing Map," in IEEE Access, vol. 11, pp. 113480-113492, 2023, doi: 10.1109/ACCESS.2023.3322450.

[31] Aamir, M., Rahman, Z., Dayo, Z.A., Abro, W.A., Uddin, M.I., Khan, I., Imran, A.S., Ali, Z., Ishfaq, M., Guan, Y., Hu, Z. (2022). A deep learning approach for brain tumor classification using MRI images. Computers and Electrical Engineering, 101: 108105. https://doi.org/10.1016/j.compeleceng.2022.108105.

[32] Ghassemi, N., Shoeibi, A., Rouhani, M. (2020). Deep neural network with generative adversarial networks pre-training for brain tumor classification based on MR images. Biomedical Signal Processing and Control, 57: 101678. https://doi.org/10.1016/j.bspc.2019.101678

[33] Anaraki, Amin Kabir, Moosa Ayati, and Foad Kazemi. "Magnetic resonan ce imaging-based brain tumor grades classification and grading via convolutional neural networks and genetic algorithms." biocybernetics and biomedical engineering 39.1 (2019): 63-74.

[34] Alanazi, M.F., Ali, M.U., Hussain, S.J., Zafar, A., Mohatram, M., Irfan, M., AlRuwaili, R., Alruwaili, M., Ali, N.H., Albarrak, A.M. (2022). Brain tumor/mass

classification framework using magnetic-resonance-imaging-based isolated and developed transfer deep-learning model. Sensors, 22(1): 372. https://doi.org/10.3390/s22010372

[35] Montaha, S., Azam, S., Rafid, A.R.H., Hasan, M.Z., Karim, A., Islam, A. (2022). Timedistributed-cnn-lstm: A hybrid approach combining CNN and LSTM to classify brain tumor on 3d MRI scans performing ablation study. IEEE Access, 10: 60039-60059. https://doi.org/10.1109/ACCESS.2022.3179577

[36] Noreen, N., Palaniappan, S., Qayyum, A., Ahmad, I., Alassafi, M.O. (2021). Brain tumor classification based on fine-tuned models and the ensemble method. Computers, Materials & Continua, 67(3). http://dx.doi.org/10.32604/cmc.2021.014158

[37] Sultan, H.H., Salem, N.M., Al-Atabany, W. (2019). Multi-classification of brain tumor images using deep neural network. IEEE Access, 7: 69215-69225. https://doi.org/10.1109/ACCESS.2019.2919122

[38] Sri, A.S., Reddy, B.V., Balakrishna, K., Akshitha, V., Kollem, S., Prasad, C.R. (2023). Detection of MRI brain tumor using customized deep learning method via web App. In 2023 International Conference on Recent Trends in Electronics and Communication (ICRTEC), Mysore, India, IEEE, pp. 1-7. https://doi.org/10.1109/ICRTEC56977.2023.10111887.